ACS OMEGA

Article

http://pubs.acs.org/journal/acsodf

Electroactive Polyhydroquinone Coatings for Marine Fouling Prevention—A Rejected Dynamic pH Hypothesis and a Deceiving Artifact in Electrochemical Antifouling Testing

Mikael Larsson,[*,†,‡] Ali Yousefi,[‡,§] Sait Elmas,[‡] Johan B. Lindén,[‡,⊥] Thomas Nann,[∥] and Magnus Nydén[†,‡]

[†]University College London, UCL—Australia, 220 Victoria Square, Adelaide, South Australia 5000, Australia

[‡]Future Industries Institute, University of South Australia, Mawson Lakes, South Australia 5095, Australia

[§]Department of Chemistry, Faculty of Science, Tarbiat Modares University, P.O. Box 14115-175, Tehran, Iran

[∥]The MacDiarmid Institute for Advanced Materials and Nanotechnology, Victoria University of Wellington, Wellington 6140, New Zealand

Supporting Information

ABSTRACT: Nanometer-thin coatings of polyhydroquinone (PHQ), which release and absorb protons upon oxidation and reduction, respectively, were tested for electrochemically induced anti-biofouling activity under the hypothesis that a dynamic pH environment would discourage fouling. Antifouling tests in artificial seawater using the marine, biofilm-forming bacterium *Vibrio alginolyticus* proved the coatings to be ineffective in fouling prevention but revealed a deceiving artifact from the reactive species generated at the counter electrode (CE), even for electrochemical bias potentials as low as |400| mV versus Ag|AgCl. These findings provide valuable information on the preparation of nanothin PHQ coatings and their electrochemical behavior in artificial seawater. The results further demonstrate that it is critical to isolate the CE in electrochemical anti-biofouling testing.

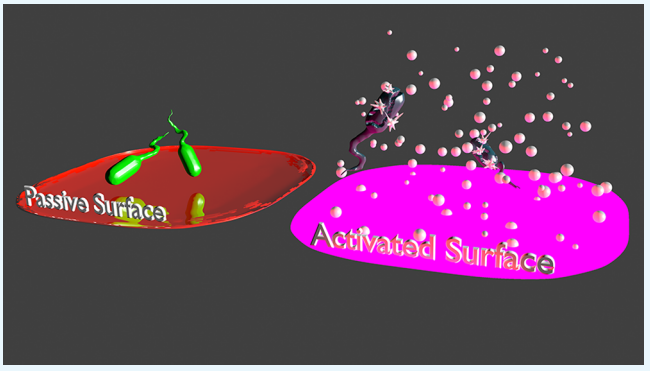

INTRODUCTION

Marine biofouling is a problem with severe economic and environmental consequences, and environmental concerns and legislation are pushing for biocide-free solutions.[1,2] Emerging "green" anti-biofouling technologies include nano-microstructured, low-adhesion, amphiphilic, zwitterionic polymers, slippery liquid-infused porous surfaces, and self-polishing coatings.[1−7] Interestingly, even if inspiration is often drawn from nature for such coatings, they are essentially designed as inactive materials. By contrast, a coating allowing for an external input of energy could be made to resemble a living system to a larger extent, for instance, by changing its physical, mechanical, or chemical state in response to a changing temperature[8,9] or an applied electric potential.[3] A dielectric elastomer deforming in response to an electric potential was reported by Shivapooja et al. with promising results.[3] The potential required was, however, very large, several kilovolts, which may limit the number of applications. Other approaches include the use of catalysts or enzymes to generate reactive oxygen species (ROS), with promising results achieved under natural conditions.[10,11]

We hypothesized that the electroactive polymer polyhydroquinone (PHQ) could be used to discourage biofouling through the formation of a dynamic pH environment at the coating interface, as PHQ is known to release and absorb protons upon oxidation and reduction, respectively.[12−14] See Scheme 1 for the structures of PHQ and the deprotonated polyquinone (PQ), as well as the hypothesized effect on interface pH.

We prepared thin coatings of PHQ on gold-coated surfaces and characterized the thickness, morphology, electrochemical behavior, and anti-biofouling properties. The biofouling studies of the marine organism *Vibrio alginolyticus*, a well-known model biofilm-forming bacterium, were used as the model system to test the anti-biofouling effect of the coatings upon oxidation and reduction with bias potentials of |400| mV versus Ag|AgCl.

Received: April 20, 2017
Accepted: August 4, 2017
Published: August 21, 2017

DOI: 10.1021/acsomega.7b00485
ACS Omega 2017, 2, 4751−4759

Scheme 1. Illustration of PHQ and PQ upon Oxidation and Reduction and the Hypothesized Effect on pH at the Coating–Water Interface

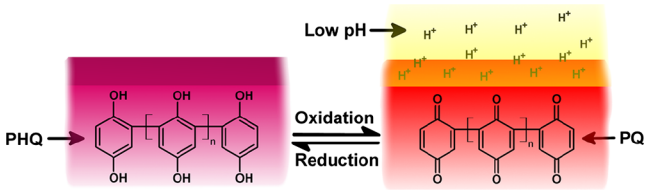

RESULTS AND DISCUSSION

PHQ Synthesis and Characterization. ^{13}C and ^{1}H NMR analysis confirmed a mixture of oxidized and reduced units in PHQ.[15] The ^{1}H NMR spectrum exhibited three characteristic broad signals at 10.00 (A), 6.78 (B), and 3.50 (C) ppm, which were assigned to phenolic protons, protons of aromatic hydroquinone units (reduced form), and protons of aliphatic (nonaromatic) quinoidal units (oxidized form), respectively (Figure S1).[15] The three broad signals at 10.35, 10.00, and 9.41 ppm indicated a twisted conformation of the polymer in dimethyl sulfoxide (DMSO).[15] From the signals at 10.35 and 10.00 ppm, which were assigned to terminal hydroquinone units, the molecular weight was estimated to be 1200 g/mol, which matched the molecular weight obtained by matrix-assisted laser desorption ionization time-of-flight (MALDI-TOF) spectrometry.

The electroactivity of PHQ in artificial seawater at pH ≈ 8.1 was confirmed using cyclic voltammetry (CV). The experiment was conducted in solution purged with N_2, using a freshly polished solid gold electrode, dip-coated with PHQ. A CV experiment is shown in Figure 1, in which the redox potentials for the transitions at the given pH agreed well with those in the literature.[13,14]

Coating Preparation and Characterization. Having established the electroactivity of PHQ in degassed seawater, coatings were prepared by spin-coating gold-coated microscopy slides with PHQ in ethanol. The coating thickness as a function of PHQ concentration was determined through ellipsometry and profilometry characterizations (Figure 2a). Coatings (10 nm) (prepared from 0.1% PHQ solutions) were deemed suitable for bacterial testing as they displayed good surface coverage and a relatively smooth surface (Figure 2b) and because it allows for electron transport across the whole coating.[16]

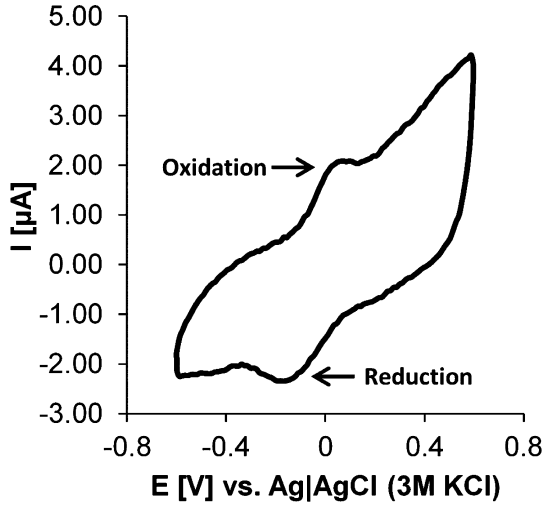

Figure 1. Cyclic voltammogram for dip-coated PHQ on a solid gold electrode in pH 8.1 artificial seawater degassed with N_2 gas. Scan speed = 100 mV/s and reference electrode (RE) = Ag|AgCl (3 M KCl).

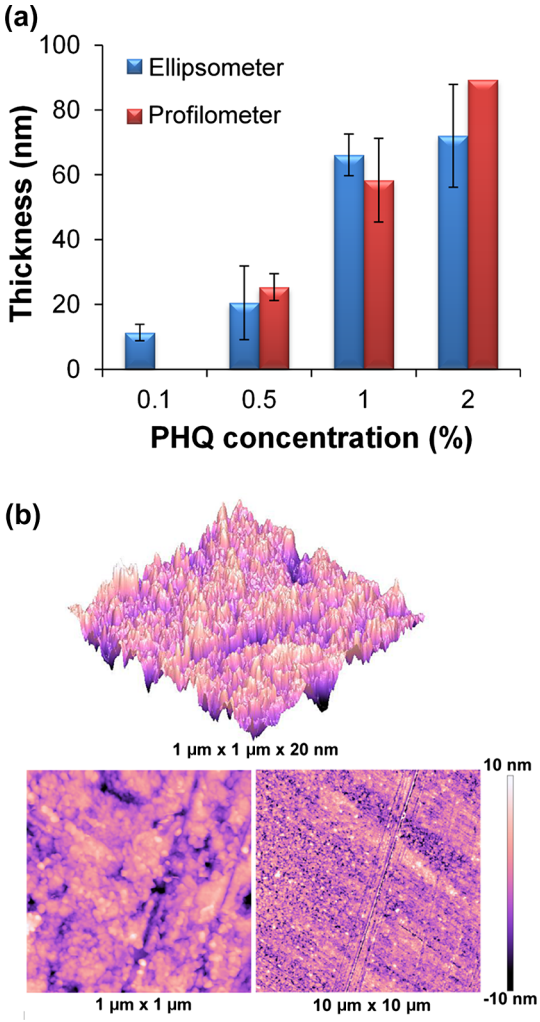

Figure 2. Coating thickness and morphology. (a) Thickness of spin-coated PHQ coatings as a function of wt % PHQ in the ethanol solution, as determined with ellipsometry and mechanical profilometry. Error bars indicate 1 standard deviation (n = 3). (b) Atomic force microscopy (AFM) height images of PHQ coatings spin-coated from 0.1% PHQ in ethanol onto a gold electrode.

The electrochemical behavior of the coatings was investigated by CV in N_2-degassed artificial seawater and 100 mM KCl. An increase in the redox currents was noted for the initial CV sweeps between −600 and +600 mV and was interpreted as a voltage-induced PHQ polymerization, leading to a more connected coating network (Figure S2). On the basis of these results, the electrochemical procedure chosen for the bacterial fouling tests was (i) five CV sweeps between −600 and +600 mV to allow for network formation and (ii) constant potentials of −400 and +400 mV in 60 s intervals to cycle between the protonated and deprotonated states of PHQ.

Anti-Biofouling and Bacterial Viability Tests. To test their anti-biofouling potential, the coatings were challenged with the marine biofilm-forming bacterium *V. alginolyticus* in artificial seawater,[17] containing 5% tryptone soy broth (TSB) as the nutrient. The coatings were evaluated for 6 and 24 h with

DOI: 10.1021/acsomega.7b00485
ACS Omega 2017, 2, 4751−4759

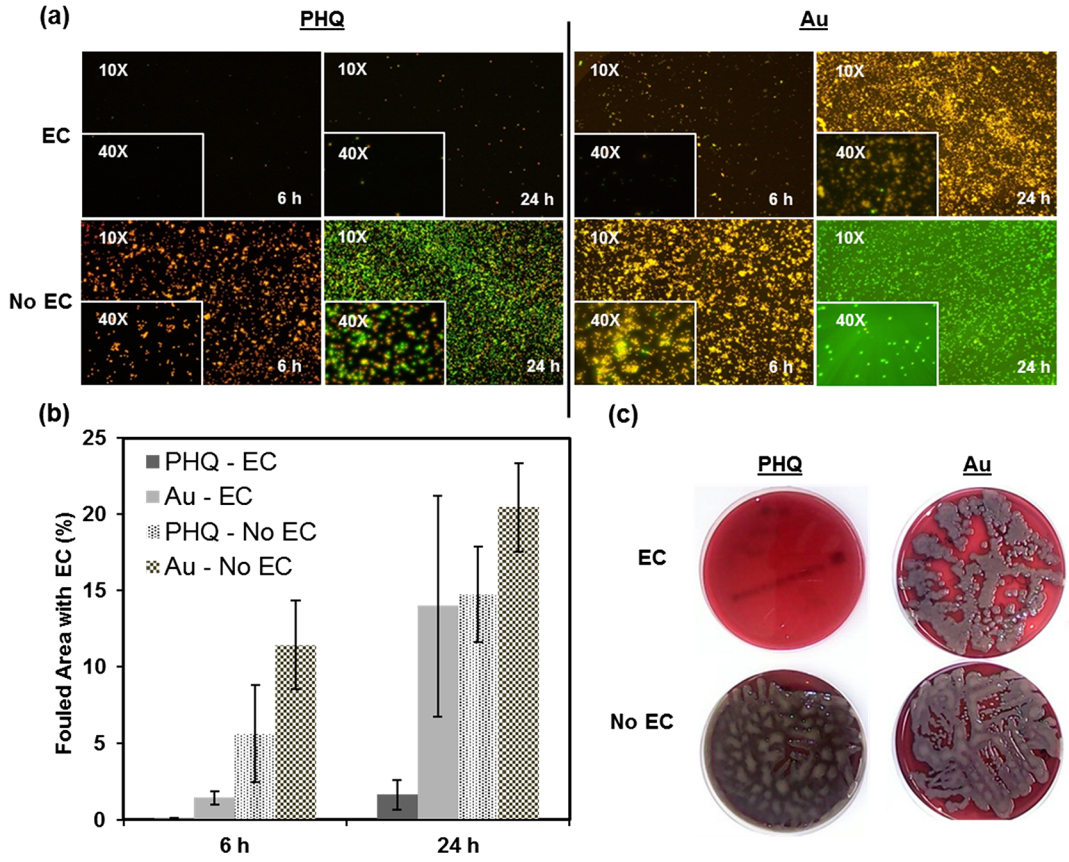

Figure 3. (a) Fluorescent microscopy images of PHQ and gold (Au) surfaces with/without EC treatment in the form of applied constant potentials after being challenged with the marine bacteria *V. alginolyticus*. The analysis times and magnifications are indicated in the figure. The bacteria were stained with the BacLight LIVE/DEAD stain. (b) Percent of the surfaces covered by fouling, as quantified from the fluorescent microscopy images. The values are presented as mean, and the error bars indicate min/max (n = 2−3) (c) Blood agar plates after streaking the bulk bacterial solutions after 6 h growth with/without EC treatment and incubation overnight; the brightness and contrast have been digitally adjusted for improved presentation.

and without electrochemical (EC) treatment. Pure gold surfaces were used as references. Fouling was very small on the PHQ surface after both 6 and 24 h when alternating between oxidizing and reducing potentials, whereas the pure gold surfaces were markedly and highly fouled after 6 and 24 h (Figure 3a,b). The reason for the strong fouling on gold after 24 h, even under alternating potentials (APs), was likely passivation by the deposition of organic materials, as supported by the X-ray photoelectron spectroscopy (XPS) analysis (Supporting Information, Figure S3). To eliminate the possibility that the antifouling effect of PHQ was due to the changes in film chemistry during the initial CV sweeps, a control experiment was carried out in which the electrochemical protocol was stopped after the five initial CV sweeps. The results revealed that further cycling was indeed necessary to prevent fouling (Figure S4).

To elucidate whether the EC treatment prevented fouling only by reducing the settlement on the surface or if the viability of the bacteria was also affected, the bacterial solution was subjected to streaking (plating out) on blood agar plates after the electrochemical process. Interestingly, the bacterial viability was greatly reduced for PHQ surfaces subjected to the electrochemical protocol, whereas less effect on viability was observed using gold with/without the EC treatment (Figure 3c).

To determine if the antibacterial action of the PHQ coating occurred only at the surface or if the whole solution was affected by the formation of antibacterial species, we investigated the effect of EC treatment of bacteria-free solutions (same procedure as above). After about 18 h of EC treatment, the solution was extracted, and bacteria were added and streaked out on blood agar plates after incubation for 90 min. As seen in Figure 4, the bacterial viability was greatly reduced in

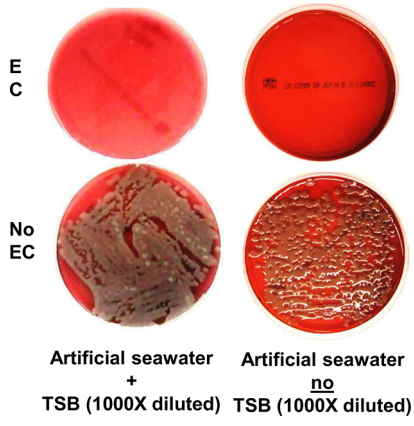

Figure 4. Blood agar plates after streaked-out bacteria added to artificial seawater and seawater and TSB (1:20), with and without EC treatment. The brightness and contrast have been digitally adjusted for improved presentation.

DOI: 10.1021/acsomega.7b00485
ACS Omega 2017, 2, 4751−4759

solutions that had been exposed to EC treatment. The same effect was seen in artificial seawater with and without TSB. We therefore conclude that antibacterial substances had been formed, thus affecting the bacteria both at the coating surface and in the solution. The attempts to identify those species and their origin are further discussed in subsequent sections.

Coating Stability and Elemental Composition. XPS and electrochemical quartz crystal microbalance with dissipation monitoring (EQCM-D) indicated that the PHQ coating remained on the surface after the EC treatment. EQCM-D analysis of PHQ coatings exposed to 6 h of EC treatment in artificial seawater revealed a decrease in the frequency and only small changes in dissipation, indicating either the slight swelling of the PHQ coating or the deposition of material onto the surface (Figure S5a). XPS analysis of coatings submerged in artificial seawater for 6 h with or without EC treatment revealed that the coatings exposed to step (i) or (ii) in the electrochemical procedure were stable, whereas those not subjected to the EC treatment seemed less stable, as seen from the Au/C ratios in Table S1. Furthermore, in the presence of TSB, the electrochemical protocol resulted in dramatically decreased frequency and increased dissipation in the EQCM-D experiment, clearly indicating the deposition of TSB onto the PHQ coating (Figure S5b). This was coherent with the new XPS signals on the gold and PHQ electrodes, in particular from calcium and phosphate, after the EC treatment in TSB containing artificial seawater. Calcium was a component of both the artificial seawater and the TSB, whereas phosphate was mainly present in the TSB. From the large increase in O/C signal ratio (Table S1), it was deemed likely that the EC treatment resulted in the deposition of some calcium phosphate on the surfaces. In conclusion, the XPS and EQCM-D results supported a PHQ network induced by the CV presweeps that resulted in a stable coating on the surface during further EC treatment. Furthermore, the XPS analysis revealed the materials deposited on the PHQ and gold surfaces during the application of constant potentials, especially in the presence of TSB.

Investigation of the Identity of the Antibacterial Species. Having established the formation of antibacterial species and that they were not degradation products of PHQ, it seemed likely that reactive species (RS) were involved, especially as they are known antibacterial agents,[10,18,19] as the oxidation/reduction of PHQ involves a radical intermediate,[20] and as the autoxidation of hydroquinone by oxygen has been reported to generate hydrogen peroxide.[21,22]

As a first attempt to characterize the electrochemical processes and generated antibacterial species, the PHQ-coated and pure gold electrodes were subjected to CV sweeps between −400 and 400 mV at a scan rate of 10 mV/s for about 20 h in artificial seawater and the presence of RS was tested with ultraviolet−visible (UV−vis) measurements using methyl orange (MO).[23] Figure 5 shows the initial and the final CV experiments for a fresh PHQ-coated electrode; the same PHQ-coated electrode used in the second experiment after rinsing with fresh artificial seawater; and a gold electrode. For the fresh PHQ-coated electrode, the cathodic reduction of oxygen started just below 0 V during the first sweep and later stabilized at −0.1 V, resulting in a peak in the current around −0.25 V. The high reduction currents remained throughout the experiment, as evident from the comparison between the 5th and 500th scans. For the pristine gold electrode, clear reduction currents were also observed but the reduction started at lower potentials and there was no peak observed around −0.25 V.

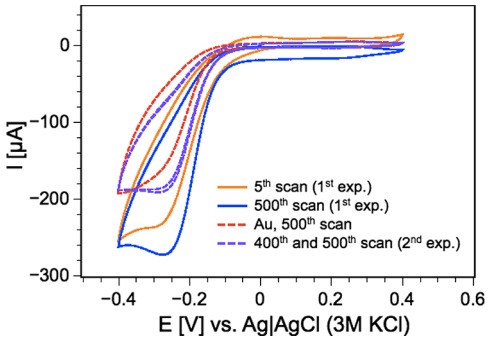

Figure 5. Cyclic voltammograms between −400 and 400 mV at 10 mV/s in pH 8.1 artificial seawater for fresh PHQ electrode (first exp.), reused, washed, and dried PHQ electrode (second exp.), and pure gold electrode (Au). RE = Ag|AgCl (3 M KCl).

The observed reduction currents likely involved oxygen, as the same reduction currents were not observed when degassed with N_2 (Figure S2). The reactions occurred for both the pure gold and the PHQ-coated electrodes, but the differences indicated that the processes and thus formed species may differ. This was later confirmed when the photometric MO assay, in which RS react with MO to change the absorbance spectrum of MO, was used to test for the presence of RS. For PHQ, it was also shown that the addition of increasing volumes of RS solution to a constant concentration of MO corresponded with an increasing shift in the spectra (Figure 6). MO solutions without RS showed the typical absorption band at 465 nm (red line). The addition of 100 μL of the RS-containing solution caused the intensity of the absorption band at 465 nm to decrease by about 25%, and a weak band emerged at 370 nm. Subsequent RS additions led gradually to an increase in the intensity of the band at 370 nm while the intensity of the band at 465 nm decreased, with close to zero intensity after the addition of 500 μL of RS (orange line). Through the series, the absorbance remained constant around 385 nm, indicating an isosbestic point at which wavelength MO and the reaction product had the same extinction coefficient. It was observed that the absorption band at 370 nm and the absorbance at the isosbestic point decreased at excess RS (dotted orange line), indicating that the RS reacted further with the product formed from the initial reaction between RS and MO. This was confirmed by measuring the UV−vis spectrum after mixing artificial seawater with MO with an equal volume containing the generated RS (excess), where it was noted that the absorbance at 370 nm and at the isosbestic point decreased over time, indicating the generation of a new species (Figure S6). The experiment was repeated for the pure gold electrode. As seen in Figure S7, no RS were detected for the gold surface in the MO assay, indicating that fewer or different species were produced at reducing currents. The MO assay also revealed that CV with the reused PHQ electrodes did not result in detectable RS production, which was also in line with the decrease in the peak current noted from the reused PHQ electrode (Figure 5). This was likely due to the chemical changes in the coating, as observed via C 1s XPS analysis (Figure S3).

To investigate the lifetime of the RS detected after CV, the MO assay was used on solutions taken directly after the EC treatment and after storage for about 5 min in open glass vials at ambient temperature. As seen in Figure 7, little to no change in MO absorbance was seen after the addition of the stored RS

DOI: 10.1021/acsomega.7b00485
ACS Omega 2017, 2, 4751−4759

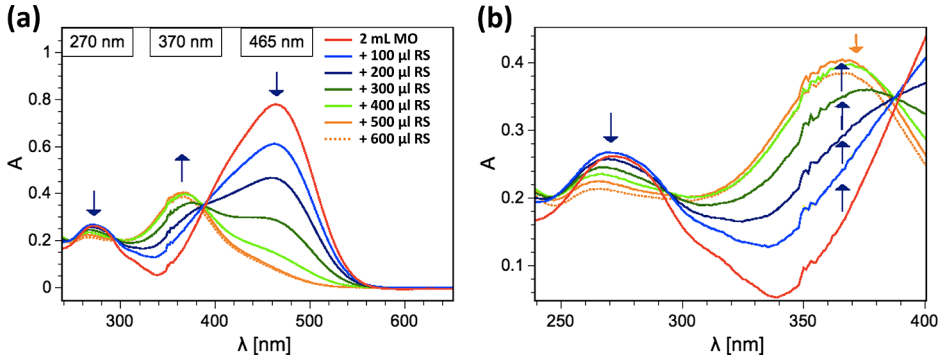

Figure 6. UV−vis spectrum of MO in artificial seawater after mixing of MO solution with different amounts of RS-containing solution, final [MO] = 5 ppm. (a) Full spectra and (b) spectrum zoomed in to clearly show the change in absorbance at 370 nm.

solution, indicating that the lifetime of the RS was shorter than 5 min.

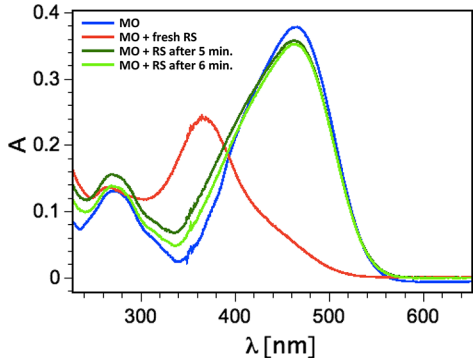

Figure 7. UV−vis spectrum of MO after mixing with fresh or stored RS solutions from CV sweeps.

It was subsequently tested if the short lifetime of the RS corresponded with a transient toxicity in an artificial seawater solution subjected to APs, as in the bacterial testing. Bacterial viability was tested in solutions taken at different times after the EC treatment. The results revealed that the viability was completely suppressed after 5 min, whereas a small viability increase was observed after 1 and 2 weeks (Figure 8). The observations indicated that the antibacterial effect noted when alternating the potential between −400 and +400 mV was not only due to the RS formed with the CV treatment but also due to other species.

The presence and type of RS in artificial seawater subjected to APs were tested with the MO assay and UV−vis spectroscopy. From the change in absorbance in the MO assay, it was concluded that RS were formed for both PHQ and pure gold surfaces (Figure 9a), with indications that the pure gold generated less and/or different species. In contrast to the CV case, the RS produced by APs remained active for a longer duration as seen in the MO spectrum of solutions stored for 30 min (Figure S8). It was further found that distinct peaks appeared in the UV spectrum after the application of APs (Figure 9b). It is known that antibacterial reactive chlorine species, for example, hypochlorite can be electrochemically generated and that they may have distinct UV signals.[24−26] It was recognized that the UV absorption signals of hypochlorite change upon protonation. We confirmed this mechanism by recording the UV−vis spectrum of hypochlorite in artificial seawater at low (pH ≈ 2.6) and high pH (pH = 8.1), see Figure 9c. As noted, the signal disappeared almost completely at pH = 8.1, whereas a distinct signal was present at 240 nm at pH ≈ 2.6. Artificial seawater was exposed to APs using pure gold and PHQ electrodes, subsequently acidified as described above, and distinct signals were observed at 230 and 235 nm for pure gold and PHQ, respectively (Figure 9d). Although blue-shifted compared to the signals from the control hypochlorite solution, the difference between these peaks could be due to a combination of absorbance from hypochlorite and other

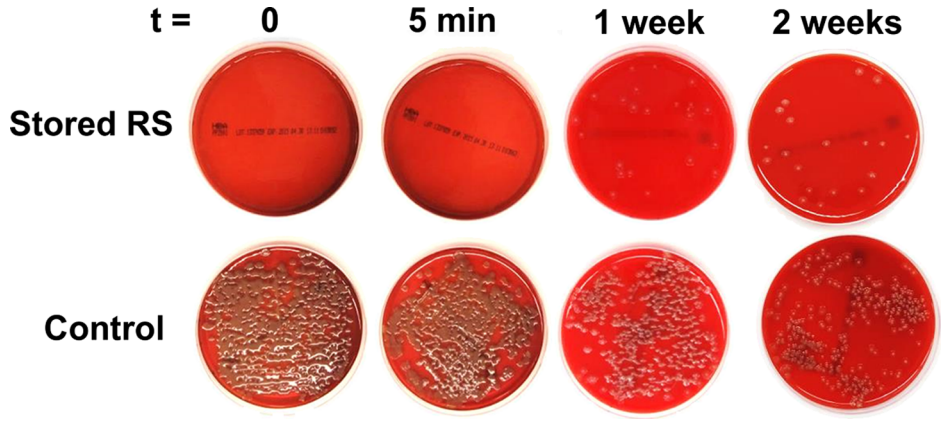

Figure 8. Blood agar plates after streaking out bacteria added to artificial seawater stored for different times after the EC treatment using a PHQ-coated electrode and APs of −400 and 400 mV (RE = AglAgCl; 3 M KCl) in 60 s intervals. The brightness and contrast have been digitally adjusted for improved presentation.

DOI: 10.1021/acsomega.7b00485
ACS Omega 2017, 2, 4751−4759

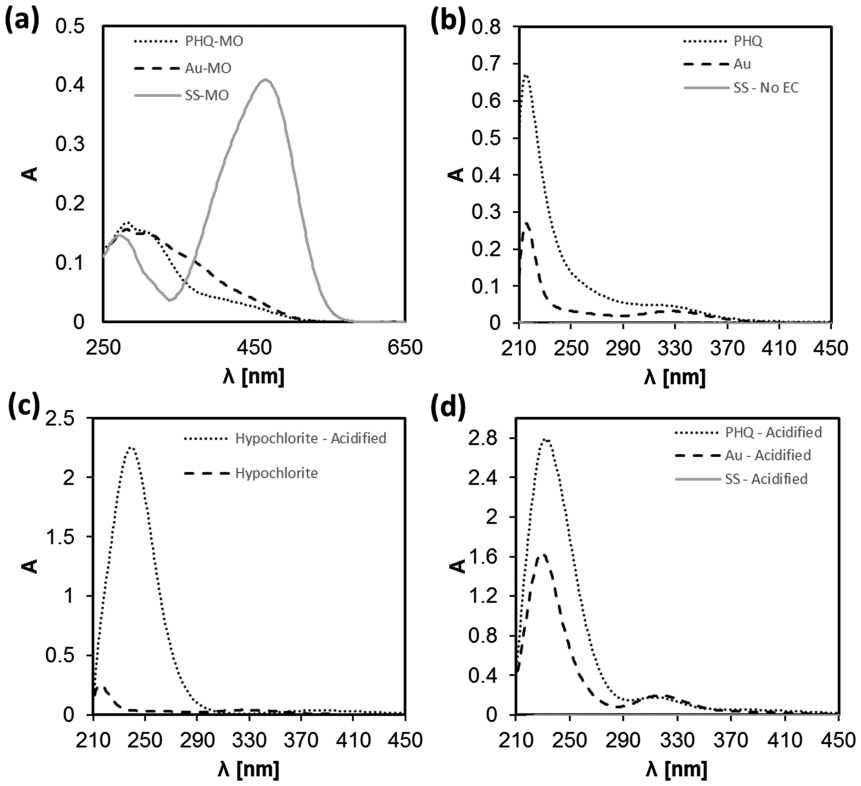

Figure 9. UV−vis spectrum of artificial seawater with and without added MO and HCl after the EC treatment using APs of −400 and 400 mV (RE = AglAgCl; 3 M KCl) in 60 s intervals on PHQ-coated (PHQ) and gold (Au) electrodes for about 17 h. Nontreated artificial seawater (SS) and artificial seawater with 0.8 μL/mL sodium hypochlorite solution (8−12.5%) were included as controls. (a) Electrochemically treated artificial seawater with added 1:1 volume of 10 ppm MO. (b) Electrochemically treated artificial seawater. (c) Artificial seawater with 0.8 μL/mL sodium hypochlorite and/or 10 μL/mL 2 M HCl (for pH ≈ 2.6). (d) Electrochemically treated artificial seawater with 10 μL/3 mL 2 M HCl (for pH ≈ 2.6).

species. In a control experiment, it was also verified that hypochlorite indeed reacted with MO (Figure S9). To conclude this section, we note that by comparing the different UV−vis spectra discussed above, a complex scenario appears, indicating a mixture of species generated from the APs applied using both the PHQ and pure gold electrodes, likely with significant amounts of hypochlorite. Figure 9 indicates that APs applied using the PHQ electrode generated more RS than using the pure gold electrode. However, it is very difficult to draw any firm conclusions regarding types and amounts of the different RS that may or may not form with the two electrodes in the current setup.

Under real-life conditions, large amounts of organic species are present and the bacterial tests were conducted in the presence of the nutrient TSB. Therefore, the EC treatment was repeated for artificial seawater with 1:20 TSB, as used in the bacterial testing. Samples were extracted at the end of both oxidizing and reducing intervals. As seen in Figure 10, no activity was observed in the MO assay and close to no changes were recorded in the UV spectra after treatment, except for slightly lower absorbance between 240 and 280 nm for samples not exposed to the EC treatment. It was thus concluded that in the presence of TSB, the formation of the RS was significantly quenched or altered. The findings are likely applicable to the presence of other organic material as well, and it seems likely that during the antibacterial tests, the generated RS reacted with both the TSB and the bacteria.

Antibacterial Species Originated from an Artifact in the Electrochemical Testing. In electrochemical testing, reactions occur at the working electrode (WE) at given

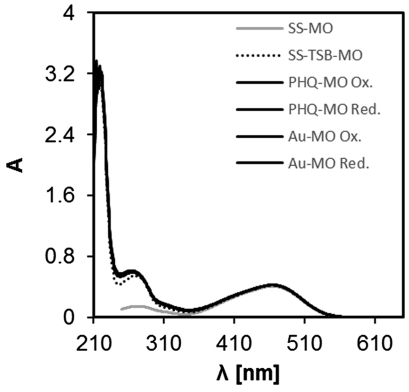

Figure 10. UV−vis spectrum of 1:1 volume ratio of 10 ppm MO and TSB-artificial seawater (1:20 volume ratio) after the EC treatment using APs of −400 and 400 mV (RE = AglAgCl; 3 M KCl) in 60 s intervals on PHQ-coated (PHQ) and gold (Au) electrodes for about 17 h. Samples were extracted and immediately added to the MO solution by the end of intervals with both oxidizing (Ox.) and reducing (Red.) potentials. Nontreated artificial seawater (SS) with MO was included as a control.

potentials, and simultaneously, balancing redox reactions occur at the counter electrode (CE). The potential at the CE is not defined; rather, the potentiostat will apply the potential bias needed to generate a current that balance the reactions at the WE. In the present work, the bias potentials applied at the WE were |400| mV versus AglAgCl. This is less than the potentials at which water is oxidized and at which chlorine gas, which subsequently form hypochlorite, is generated from saline water.

DOI: 10.1021/acsomega.7b00485
ACS Omega 2017, 2, 4751−4759

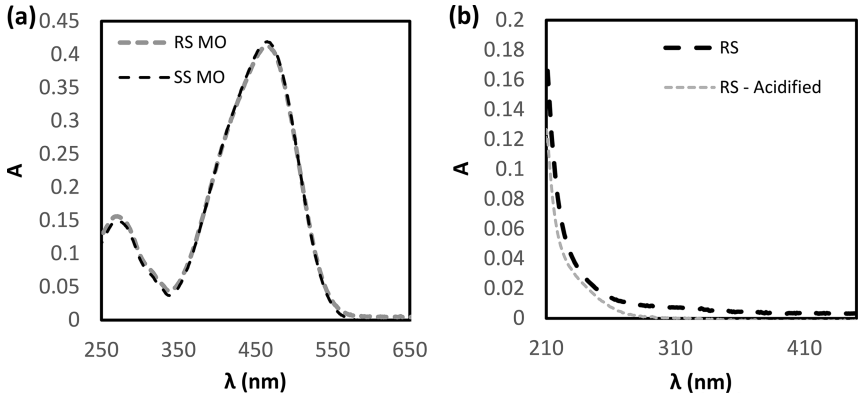

Figure 11. UV−vis spectrum after the EC treatment for about 17 h using APs of −400 and 400 mV (RE = AgIAgCl; 3 M KCl) in 60 s intervals and PHQ-coated WE electrodes, with the CE separated from the solution using a glass frit. (a) Artificial seawater with 1:1 volume ratio of 10 ppm MO added after the EC treatment and nontreated artificial seawater (SS) with MO included as a control. (b) Electrochemically treated artificial seawater with and without 10 μL/3 mL 2 M HCl (for pH ≈ 2.6).

The nominal oxidation potential for water splitting is 1.23 V [vs normal hydrogen electrode (NHE)], and commercial electrolyzers operate at potentials above 1.8 V (vs NHE).[27]

Given the low applied voltages at the WE, it was not expected that hypochlorite and RS were from the reactions at the CE, and no gas formation was visually observed. However, to test if the RS were generated at the CE, it was separated from the test solution using a glass tube with a frit during the application of APs to a PHQ-coated WE. No RS was detected using the MO assay, as seen from the lack of change in the MO spectra compared to those of the control solution (Figure 11a), and only slight absorbance at short wavelengths, which did not change upon acidification, was detected for the solution without MO (Figure 11b). Antibacterial experiments were repeated with the CE separated from the solution with a glass frit, applying APs to a PHQ-coated WE for 6 h. No reduction in biofouling was observed for the PHQ-coated electrode subjected to APs compared to the control without the application of APs (Figure S10). In fact, it was hinted that the control was less fouled, but the differences in how the bacteria distributed on the surface made further conclusions difficult.

It was concluded that the observed antifouling and antibacterial effects were due to an artifact from the species generated at the CE, even under applied bias potentials as low as |400| mV versus AgIAgCl. The results clearly highlight the caution needed in the interpretation of results when using electrochemistry in a biological setting and the need to separate the CE from the WE in such studies.

CONCLUSIONS

We prepared and characterized thin coatings of PHQ and tested for anti-biofouling under alternating oxidizing and reducing potentials of |0.4 V| versus AgIAgCl. The hypothesis was that proton release and uptake of the material upon oxidation and reduction, respectively, would discourage biofouling through a dynamic pH environment at the coating−water interface. Initial observations indicated antifouling and biocidal effects of the electroactivated coatings, but further investigations revealed that the effects were an artifact from the RS generated at the CE. Thus, the hypothesis was rejected. Nonetheless, the results provide thorough information on the preparation of PHQ coatings and their electrochemical behavior in seawater. The results further act to demonstrate the great care that needs to be taken in the setup and interpretation of results when combining electrochemistry and biological studies, a field that will likely emerge further as functional smart materials evolve.

METHODS

Materials. Arbutin (≥98%), hydroquinone (ReagentPlus), deuterated dimethyl sulfoxide (DMSO-d_6), glycerol (99%), and sea salts were bought from Sigma-Aldrich. Ethanol (100% undenatured), disodium hydrogen phosphate, sodium dihydrogen phosphate, sodium hypochlorite solution (8−12.5%), and potassium chloride were bought from Chem-Supply. KCl was purified by calcination (8 h at 550 °C), recrystallization, and a second calcination (8 h at 550 °C). Soybean peroxidase was bought from Bio-Research Products Inc. Columbia horse blood agar plates and TSB were acquired from Oxoid. Artificial seawater was prepared from the sea salts from Sigma-Aldrich (38 g/L). Deionized water was used for the bacterial testing and Milli-Q water for all other experiments.

PHQ Synthesis and Characterization. PHQ was enzymatically synthesized as described previously[13] and stored under N_2. NMR spectra were recorded at room temperature with a Bruker AVANCE III spectrometer in DMSO-d_6. The chemical shifts δ are referred to TMS (tetramethylsilane) as a standard and were assigned as ^{1}H NMR (300 MHz, DMSO-d_6, δ): 3.50 (br s, 2H, quinone H), 6.78 (br s, 2H, hydroquinone H), 10.00 (br s, 2H, hydroquinone OH); ^{13}C APT NMR (75 MHz, DMSO-d_6, δ): 155.40 (2C, quaternary C), 150.62 (2C, quaternary C), 146.72 (2C, quaternary C), 122.47−121.15 (2C, hydroquinone CH), 119.10−117.20 (2C, quinone CH). MALDI-TOF characterization of molecular weight was conducted on a Bruker ultrafleXtreme MALDI/TOF/TOF equipped with a 2 kHz laser and using *trans*-2-[3-(4-*tert*-butylphenyl)-2-methyl-2-propenylidene]malononitrile as the matrix.

PHQ Coating Preparation. PHQ was dissolved in ethanol at different concentrations and spin-coated at 2000 rpm on gold-coated microscopy slides with a titanium sublayer at room temperature (Deposition Research Lab. Inc.) or cut 1 × 1 cm silicon wafers (WRS). Solid gold electrodes were polymer-coated by submersion for 10 min in 0.1% PHQ in ethanol, followed by gentle drying with N_2.

Thickness and Surface Morphology Characterization. The coating thickness was characterized in triplicate on the

DOI: 10.1021/acsomega.7b00485
ACS Omega 2017, 2, 4751−4759

silicon wafers with a variable angle spectroscopic ellipsometer (VASE) and WVASE32 software (J.A. Woollam Co., Inc.) and a DektakXT profilometer with a 12.5 μm stylus (Bruker) under a 3 mg load. The coating surface morphology was investigated using ScanAsyst in air on a NanoScope MultiMode 8 AFM (Bruker) with a NanoScope V controller.

Electrochemical Characterization, Activation, and Reactive Species Detection. Electrochemical experiments were performed using potentiostats from Zahner and Autolab, with three-electrode setups. For bacterial tests, the WE was a gold-coated microscopy slide, the CE and RE were a rolled-up 82 × 82 wires/inch platinum mesh and a silver wire (Ag pseudoref), respectively (Goodfellow). For dip-coated coatings, solid gold, solid platinum, and a AglAgCl (3 M KCl) RE were used as WE, CE, and RE, respectively (CH Instruments Inc.). For EQCM-D experiments, the gold QCM sensor (Q-Sense) was the WE, a platinum plate (Q-Sense) was the CE, and a Dri-Ref AglAgCl (3 M KCl) electrode (World Precision Instruments, Inc.) was the RE. The electrolytes were 0.1 M KCl or artificial seawater. For the generation of RS during CV, an area of about 2 × 2.5 cm of the WE was submerged in 20 mL of artificial seawater and the potential was cycled between 400 and −400 mV at a scan rate of 10 mV/s for 20 h. For the generation of RS during the application of APs of −400 and +400 mV in 60 s intervals for 16−17 h, an area of about 4 × 2.5 cm was submerged in 30 mL of artificial seawater with or without 1:20 TSB. The presence of RS was detected as follows: the requisite amount of electrolyte solution containing RS was added to 10 ppm MO solution, followed by the addition of artificial seawater for a final MO concentration of 5 ppm. Furthermore, direct UV−vis absorbance on solution without MO was used, with or without acidification using 10 μL/3 mL 2 M HCl. In all cases, UV−vis absorbance was measured on a Varian Cary 300 Bio UV−vis spectrometer using a quartz cuvette and the presence of RS was evaluated from the changes in the UV−vis spectrum of MO or absorbance of the solution without MO. EC treatment in bacterial tests refers to the continuous application of APs of −400 and +400 mV in 60 s intervals. In experiments where the contribution from the species generated at the CE was to be eliminated, the CE was placed in a glass tube with a frit in the submerged end and the tube was filled with the electrolyte solution. All potentials are reported versus the used RE ≈ AglAgCl in the electrolytes used.

QCM Analysis. The analyses were conducted on spin-coated coatings using an E4 Quartz Crystal Microbalance, gold sensors, and standard or electrochemical modules (Q-Sense) at a flow rate of 0.1 mL/min. Electrochemistry was conducted without flow.

X-ray Photoelectron Spectroscopy. The samples were taken out of the solution, briefly rinsed with Milli-Q water, and dried with nitrogen gas just before being loaded into the instrument. The analyses were undertaken in duplicates using monochromatized Al Kα X-rays (1486.7 eV) at a power of 225 W on a Kratos Axis Ultra spectrometer (160 eV analyzer pass energy for survey scans and 20 eV for high-resolution scans). The analysis spot size was ∼300 × 700 μm. Data analysis was conducted using a CasaXPS.

Bacterial Testing. The PHQ-coated surfaces (from here on referred to as PHQ surfaces or electrodes) and bare gold surfaces (from here on referred to as gold surfaces or electrodes) were challenged with *V. alginolyticus* (strain 130) with/without EC treatment as follows: From −20 °C, bacteria in TSB with 15% glycerol were cultured overnight at 37 °C on Columbia horse blood agar plates (Oxoid). One colony was picked and grown under aerobic conditions in TSB overnight at 37 °C. The OD_{600} was adjusted to 0.1 (≈2.5 × 10^6 colony forming units/mL) in 1:20 TSB to artificial seawater. The bacteria were added to Teflon block electrochemical cells with the PHQ-coated, or pure gold, WE in vertical orientation, an exposed area of 0.8 cm^2, a volume of 1 mL. The same bacterial suspension was split between the sample subjected to the EC treatment and the control. All experiments were conducted at room temperature. Five CV presweeps were conducted for samples exposed to the EC treatment, followed by the application of APs of −400 and +400 mV in 60 s intervals through 6 or 24 h of the experiments. Subsequently, the medium was gently replaced with BacLight LIVE/DEAD solution (Life Technologies) containing 1.5 μL/mL component A and B. The samples were incubated for 30 min before being washed three times by gentle immersion in deionized water. Images were recorded for hydrated samples at 10× and 40× magnification using a green-red dual pass filter on an Eclipse Ni-U fluorescent microscope. More than three spots were analyzed per sample at each magnification. ImageJ was used to quantify the fouled area of samples by analyzing three or more images (locations) per sample and to calculate the average. The viability of bacteria in the bulk solution after the experiments was evaluated by streaking out 100 μL of solution on Columbia horse blood agar plates (Oxoid) at 1000× or 10 000× dilutions, followed by incubation overnight. The effect of solution subjected to the EC treatment on the viability of fresh bacteria was assessed as follows: Artificial seawater with and without TSB was exposed to the EC treatment using a gold or PHQ electrode for 16−19 h. Subsequently, bacterial solutions grown in TSB overnight were diluted 25× with artificial seawater and were added to the solutions subjected to the EC treatment, for a total dilution of 1000× or 10 000×. The samples were incubated for 90 min before streaking on blood agar plates and incubation overnight.

■ ASSOCIATED CONTENT

Supporting Information

The Supporting Information is available free of charge on the ACS Publications website at DOI: 10.1021/acsomega.7b00485.

^{1}H-NMR spectrum of the synthesized PHQ, cyclic voltammetry in artificial seawater on coatings prepared from 0.1% PHQ in ethanol, XPS C 1s characterization of coatings and gold surfaces, bacterial testing for coatings exposed only to the initial five CV sweeps, EQCM-D analysis of PHQ coatings during the EC treatment, further degradation of MO-RS product after CV, CV experiment for a pure gold electrode, maintained activity of reactive species over time after the application of APs, activity of hypochlorite against MO, and bacterial testing with the counter electrode separated by a glass frit (PDF)

■ AUTHOR INFORMATION

Corresponding Author

*E-mail: larsson.mikael@gmail.com (M.L.).

ORCID

Mikael Larsson: 0000-0002-6755-8418

Sait Elmas: 0000-0002-1235-1436

Thomas Nann: 0000-0002-2723-6553

DOI: 10.1021/acsomega.7b00485
ACS Omega 2017, 2, 4751−4759

Present Address

[⊥]Research Institutes of Sweden, Division of Bioscience and Materials, Chemistry, Materials and Surfaces, Brinellgatan 4, 50462 Borås, Sweden.

Notes

The authors declare no competing financial interest.

■ ACKNOWLEDGMENTS

This research was supported by the Australian Government through the Australian Research Council's Discovery Projects funding scheme (project DP160102356). The authors thank Christopher Bassel and Dr. Taryn Guinan, Future Industries Institute, University of South Australia, for XPS and MALDI-TOF measurements, respectively.

■ REFERENCES

(1) Kirschner, C. M.; Brennan, A. B. Bio-Inspired Antifouling Strategies. *Annu. Rev. Mater. Res.* **2012**, *42*, 211−229.

(2) Callow, J. A.; Callow, M. E. Trends in the development of environmentally friendly fouling-resistant marine coatings. *Nat. Commun.* **2011**, *2*, 244.

(3) Shivapooja, P.; Wang, Q.; Orihuela, B.; Rittschof, D.; López, G. P.; Zhao, X. Bioinspired Surfaces with Dynamic Topography for Active Control of Biofouling. *Adv. Mater.* **2013**, *25*, 1430−1434.

(4) Zhao, N.; Wang, Z.; Cai, C.; Shen, H.; Liang, F.; Wang, D.; Wang, C.; Zhu, T.; Guo, J.; Wang, Y.; Liu, X.; Duan, C.; Wang, H.; Mao, Y.; Jia, X.; Dong, H.; Zhang, X.; Xu, J. Bioinspired Materials: from Low to High Dimensional Structure. *Adv. Mater.* **2014**, *26*, 6994−7017.

(5) Banerjee, I.; Pangule, R. C.; Kane, R. S. Antifouling Coatings: Recent Developments in the Design of Surfaces That Prevent Fouling by Proteins, Bacteria, and Marine Organisms. *Adv. Mater.* **2011**, *23*, 690−718.

(6) Wang, P.; Zhang, D.; Lu, Z. Slippery liquid-infused porous surface bio-inspired by pitcher plant for marine anti-biofouling application. *Colloids Surf., B* **2015**, *136*, 240−247.

(7) Quintana, R.; Jańczewski, D.; Vasantha, V. A.; Jana, S.; Lee, S. S. C.; Parra-Velandia, F. J.; Guo, S.; Parthiban, A.; Teo, S. L.-M.; Vancso, G. J. Sulfobetaine-based polymer brushes in marine environment: Is there an effect of the polymerizable group on the antifouling performance? *Colloids Surf., B* **2014**, *120*, 118−124.

(8) Ista, L. K.; Pérez-Luna, V. H.; López, G. P. Surface-Grafted, Environmentally Sensitive Polymers for Biofilm Release. *Appl. Environ. Microbiol.* **1999**, *65*, 1603−1609.

(9) Cordeiro, A. L.; Pettit, M. E.; Callow, M. E.; Callow, J. A.; Werner, C. Controlling the adhesion of the diatom Navicula perminuta using poly(N-isopropylacrylamide-co−N-(1-phenylethyl) acrylamide) films. *Biotechnol. Lett.* **2010**, *32*, 489−495.

(10) Natalio, F.; André, R.; Hartog, A. F.; Stoll, B.; Jochum, K. P.; Wever, R.; Tremel, W. Vanadium pentoxide nanoparticles mimic vanadium haloperoxidases and thwart biofilm formation. *Nat. Nanotechnol.* **2012**, *7*, 530−535.

(11) Olsen, S. M.; Kristensen, J. B.; Laursen, B. S.; Pedersen, L. T.; Dam-Johansen, K.; Kiil, S. Antifouling effect of hydrogen peroxide release from enzymatic marine coatings: Exposure testing under equatorial and Mediterranean conditions. *Prog. Org. Coat.* **2010**, *68*, 248−257.

(12) Yamamoto, K.; Asada, T.; Nishide, H.; Tsuchida, E. The Preparation of Poly(dihydroxyphenylene) through the Electro-Oxidative Polymerization of Hydroquinone. *Bull. Chem. Soc. Jpn.* **1990**, *63*, 1211−1216.

(13) Wang, P.; Amarasinghe, S.; Leddy, J.; Arnold, M.; Dordick, J. S. Enzymatically prepared poly(hydroquinone) as a mediator for amperometric glucose sensors. *Polymer* **1998**, *39*, 123−127.

(14) Nakano, K.; Hirayama, G.; Toguchi, M.; Nakamura, K.; Iwamoto, K.; Soh, N.; Imato, T. Poly(hydroquinone)-coated electrode for immobilizing of 5′-amine functioned capture probe DNA and electrochemical response to DNA hybridization. *Sci. Technol. Adv. Mater.* **2006**, *7*, 718.

(15) Madkour, T. M. Chemistry of Polymerization Products of p-Benzoquinone. 13C NMR and Molecular Dynamics Study. *Polym. J.* **1997**, *29*, 670−677.

(16) Yan, H.; Bergren, A. J.; McCreery, R.; Della Rocca, M. L.; Martin, P.; Lafarge, P.; Lacroix, J. C. Activationless charge transport across 4.5 to 22 nm in molecular electronic junctions. *Proc. Natl. Acad. Sci. U.S.A.* **2013**, *110*, 5326−5330.

(17) Okochi, M.; Nakamura, N.; Matsunaga, T. Electrochemical control of bacterial cell accumulation on submerged glass surfaces. *Clean Technol. Environ. Policy* **1998**, *1*, 53−59.

(18) Li, Y.; Zhang, W.; Niu, J.; Chen, Y. Mechanism of Photogenerated Reactive Oxygen Species and Correlation with the Antibacterial Properties of Engineered Metal-Oxide Nanoparticles. *ACS Nano* **2012**, *6*, 5164−5173.

(19) Fang, F. C. Antimicrobial Actions of Reactive Oxygen Species. *mBio* **2011**, *2*, No. e00141-11.

(20) Yamamoto, T.; Kimura, T.; Shiraishi, K. Preparation of π-Conjugated Polymers Composed of Hydroquinone, p-Benzoquinone, and p-Diacetoxyphenylene Units. Optical and Redox Properties of the Polymers. *Macromolecules* **1999**, *32*, 8886−8896.

(21) Radel, R. J.; Sullivan, J. M.; Hatfield, J. D. Catalytic oxidation of hydroquinone to quinone using molecular oxygen. *Ind. Eng. Chem. Prod. Res. Dev.* **1982**, *21*, 566−570.

(22) James, T. H.; Snell, J. M.; Weissberger, A. Oxidation Processes. XII. 1 The Autoxidation of Hydroquinone and of the Mono-, Di- and Trimethylhydroquinones. *J. Am. Chem. Soc.* **1938**, *60*, 2084−2093.

(23) Minitha, C. R.; Pandian, R.; Amirthapandian, S.; Kumar, R. T. R. Unexpected production of singlet oxygen by sub-micron cerium oxide particles and enhanced photocatalytic activity against methyl orange. *RSC Adv.* **2015**, *5*, 56982−56986.

(24) Elmas, S.; Ambroz, F.; Chugh, D.; Nann, T. Microfluidic Chip for the Photocatalytic Production of Active Chlorine. *Langmuir* **2016**, *32*, 4952−4958.

(25) Abdessemed, A.; Djebbar, K. E.; El-Kalliny, A. S.; Sehili, T.; Nugteren, H.; Appel, P. W. Water Treatment Combined Chlorine (Monochloramine) Degradation using Direct Photolysis and Homogeneous Photocatalysis (UV/H2O2, UV/NaOCl) with a Medium Pressure (MP) Lamp as a Source of UV. *Int. J. Chem. React. Eng.* **2014**, *12*, 671.

(26) Paprocki, A.; dos Santos, H. S.; Hammerschitt, M. E.; Pires, M.; Azevedo, C. M. N. Ozonation of azo dye acid black 1 under the suppression effect by chloride ion. *J. Braz. Chem. Soc.* **2010**, *21*, 452−460.

(27) Wei, S.; Qi, K.; Jin, Z.; Cao, J.; Zheng, W.; Chen, H.; Cui, X. One-Step Synthesis of a Self-Supported Copper Phosphide Nanobush for Overall Water Splitting. *ACS Omega* **2016**, *1*, 1367−1373.

DOI: 10.1021/acsomega.7b00485
ACS Omega 2017, 2, 4751−4759